NASA/CR- $-\varsigma' 7-$ 207812

ROSAT OBSERVATIONS OF A NEW X-RAY TRANSIENT IN THE SMALL MAGELLANIC CLOUD

GEORGE W. CLARK,[1] RONALD A. REMILLARD, AND JONATHAN W. WOO[2]

Center for Space Research, Massachusetts Institute of Technology, Cambridge, MA 02139

ABSTRACT

We describe *ROSAT* observations of a new X-ray transient and its probable optical companion in the Small Magellanic Cloud. The transient, designated RX J0117.6−7330, appeared at a position ∼5′ southeast of the X-ray pulsar, SMC X-1, in 1992 October 1–2 PSPC observations centered on the pulsar. It was detected again in a similar observation 246 days later at a counting rate diminished by a factor of 270, which corresponds to an average *e*-folding decay time of 44 days. No periodic pulsations have been detected. The average 1992 flux level would be produced by a source radiating isotropically with a luminosity of 1.6×10^{37} $(D/50 \text{ kpc})^2$ ergs s^{-1} in the energy range 0.2–2.5 keV. The 5″ radius positional error circle includes the probable optical counterpart in the form of a magnitude $V = 14.2$ star with the spectral characteristics of type Be.

Subject headings: galaxies: Magellanic Clouds — novae, cataclysmic variables —
stars: individual (RX J0117.6−7330) — X-rays: binaries — X-rays: stars

1. INTRODUCTION

Of the 71 transient X-ray binaries containing neutron stars or black holes listed in a 1992 catalog of high- and low-mass X-ray binaries (van Paradijs 1995), three are in the Small Magellanic Cloud (SMC) and two are in the Large Magellanic Cloud (LMC), of which one is a 69 ms pulsar. The optical companions have V magnitudes in the range 14–17 mag, and all have been characterized as early-type giants or subgiants of type Be. *ROSAT* observations have revealed additional Magellanic transients: a pulsar in the LMC with a period of 4.0635 s and a Be-type companion (Schmidtke et al. 1995), and three transients with certain or likely Be-type companions in the SMC (Kahabka & Pietsch 1996), of which one is a 2.7632 s pulsar with an unusually soft X-ray spectrum (Hughs 1994). All of these transients are believed to be neutron stars in binary systems in which episodes of enhanced accretion cause outbursts of X-ray emission that last from weeks to months.

Among the galactic transients is a subclass of nonpulsing X-ray sources with masses that exceed 3.0 $M_{\odot}$, the causality limit on the mass of a neutron star. These objects (see Tanaka & Lewin 1995), the so-called black hole X-ray novas (BHXN), typically have an "ultrasoft" spectrum characterized by a much higher ratio of the flux between 1 and 3 keV to the flux between 3 and 10 keV compared to that for pulsars, a high-energy tail detectable in some cases to more than 100 keV, a maximum luminosity of the order of 10^{38} ergs s^{-1}, and *e*-folding decay times in the range 30–60 days. They are strongly concentrated toward the galactic plane, with a mean value of $|b^{\text{II}}| < 5°$, and their companions have all been identified as late-type dwarfs or subgiants. None have yet been observed in the Magellanic Clouds.

In this Letter, we describe observations of a new X-ray transient in the SMC (Clark, Remillard, & Woo 1996). Spectroscopy of its probable optical counterpart (Charles, Southwell, & O'Donoghue 1996) has shown a spectrum with the characteristics of a massive Be star, which makes it likely

that the transient is another example of an accretion-powered neutron star with a Be-type companion. At the same time, the transient has some of the X-ray characteristics of a BHXN.

2. OBSERVATIONS AND DATA ANALYSIS

Observations were made with the Position Sensitive Proportional Counter (PSPC) at the focal plane of the X-Ray Telescope on board the *ROSAT* X-Ray Observatory. Details of the observatory have been described by Trümper (1983), Pfeffermann et al. (1987), and Aschenbach (1988).

The observations were centered on the binary X-ray pulsar SMC X-1 and were carried out during 1991 October 7.2–8.1, 1992 September 30.7 to October 2.6, and 1993 June 3.0–4.4 with total exposures of 16955 s, 8984 s, and 11864 s, respectively. No vignetting corrections were made because the transient image was near the center of the field of view in the region of flat response. (SMC X-1 was in eclipse during most of the 1992 and 1993 observations.)

Counting rate contour maps of the central region of the XRT/PSPC images from the three observations are displayed in Figure 1. The 1991 image shows SMC X-1 at the center and the coronal X-ray star, HD 8191, identified by Seward & Mitchell (1981). The transient source appears in the 1992 image as a bright object at a position approximately 5′ southeast SMC X-1. The 1993 image shows the transient source with greatly diminished intensity. We adopt the designation RX J0117.6−7330 for this object.

2.1. *Position and Optical Identification*

The angular separations of the transient from SMC X-1 and HD 8191 in the 1992 X-ray image are 293″.6 ± 1″.1 and 404″.7 ± 1″.4, respectively. The coordinates of the point that lies at these angular separations from the optical positions of Sk 160 and HD 8191, derived from the Digital Sky Survey (DSS), are $01^{\text{h}}17^{\text{m}}40^{\text{s}}.12 \pm 1^{\text{s}}.17$, $-73°30'48'' \pm 5''$. Figure 2 (Plate L13) is a 2′ × 2′ portion of the DSS, with the position of the transient indicated as a 90% confidence error circle centered at the derived position with a radius of 5″. The error circle encloses a blue star of magnitude $V \approx 14$. Its position, derived from the DSS, is $01^{\text{h}}17^{\text{m}}40^{\text{s}}.30 \pm 0^{\text{s}}.23$, $-73°30'50''.3 \pm 1''$.

[1] Department of Physics, Massachusetts Institute of Technology, Cambridge, MA 02139.

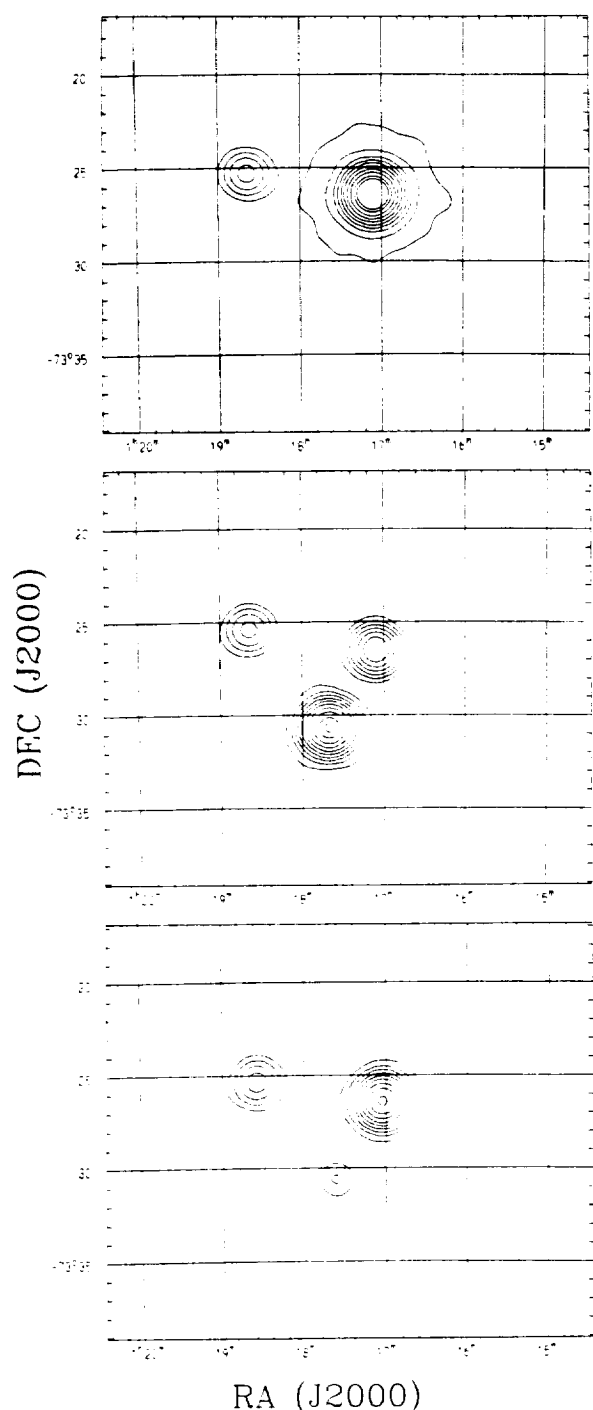[2] Present address: Harvard-Smithsonian Center for Astrophysics, Cambridge, MA 02138.

FIG. 1.—Contour maps of smoothed counts per unit area in the central region of the *ROSAT* images recorded in three observations of SMC X-1. Contour levels differ by factors of 2. *Top*: 1991 HD 8191 ~7' east of SMC X-1. *Middle*: 1992 transient 5' southeast of SMC X-1. *Bottom*: 1993 transient faded.

Figure 3 displays the average of two spectra of the star obtained on 1996 May 17 and 18 with the Cassegrain spectrograph (3" slit) at the Cerro Tololo Inter-American Observatory (CTIO) 1.5 m telescope. It shows the strong, narrow emission lines of Hα and Hβ on the blue continuum of a star of magnitude $V = 14.2$, as reported by Charles et al. (1996). and Hδ and higher order H lines in absorption—all characteristics of a Be star.
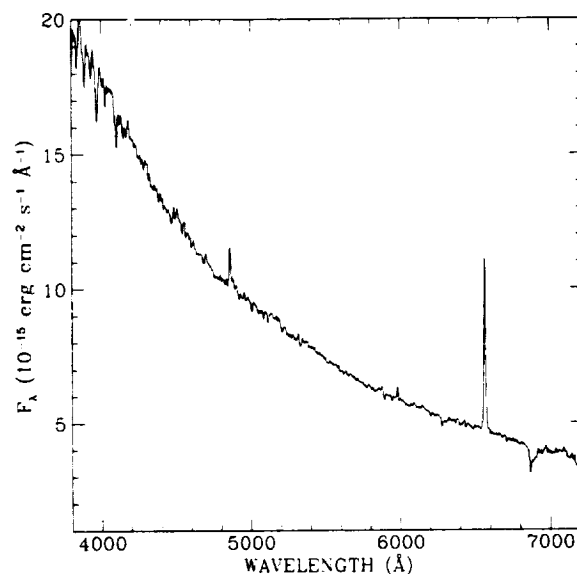

FIG. 3.—Spectrum of the candidate optical companion of RX J0117.6−7330.

2.2. *Variability*

For timing analysis, the event times were converted to barycenter times. Events within a circle of radius 1.'67 centered on the transient's image were counted as source plus background. Background rates were determined from the numbers of events in a concentric annulus of inner and outer radii 1.'67 and 2.'5, respectively. We found no statistically significant variations in the average background rates, which were equal to 0.9% and 58% of the source plus background rates in the 1992 and 1993 observations, respectively.

The light curve from the 1992 observation is shown in Figure 4a as a plot of average background-subtracted count rates in 18 subsets of the data comprised of the events from continuous 400 s portions of the exposure. The subset duration was set equal to the approximate period of the controlled wobble in the pointing direction of the spacecraft in order to minimize
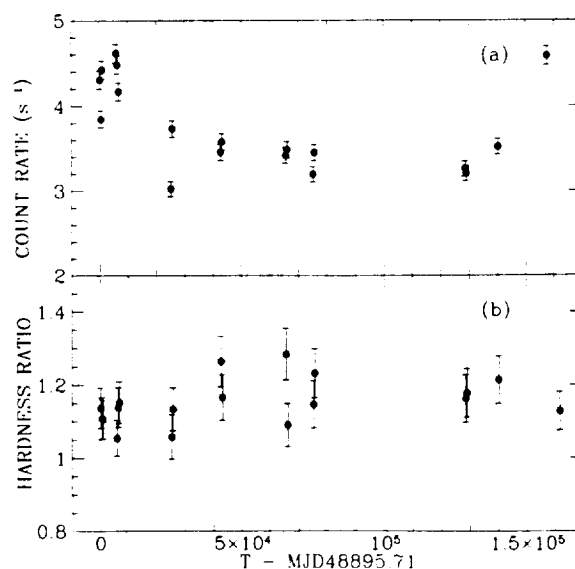

FIG. 4.—(*a*) Count rates and (*b*) hardness ratio of RX J0117.6−7330 during the 1992 observation, averaged in 400 s intervals and plotted against MJD.
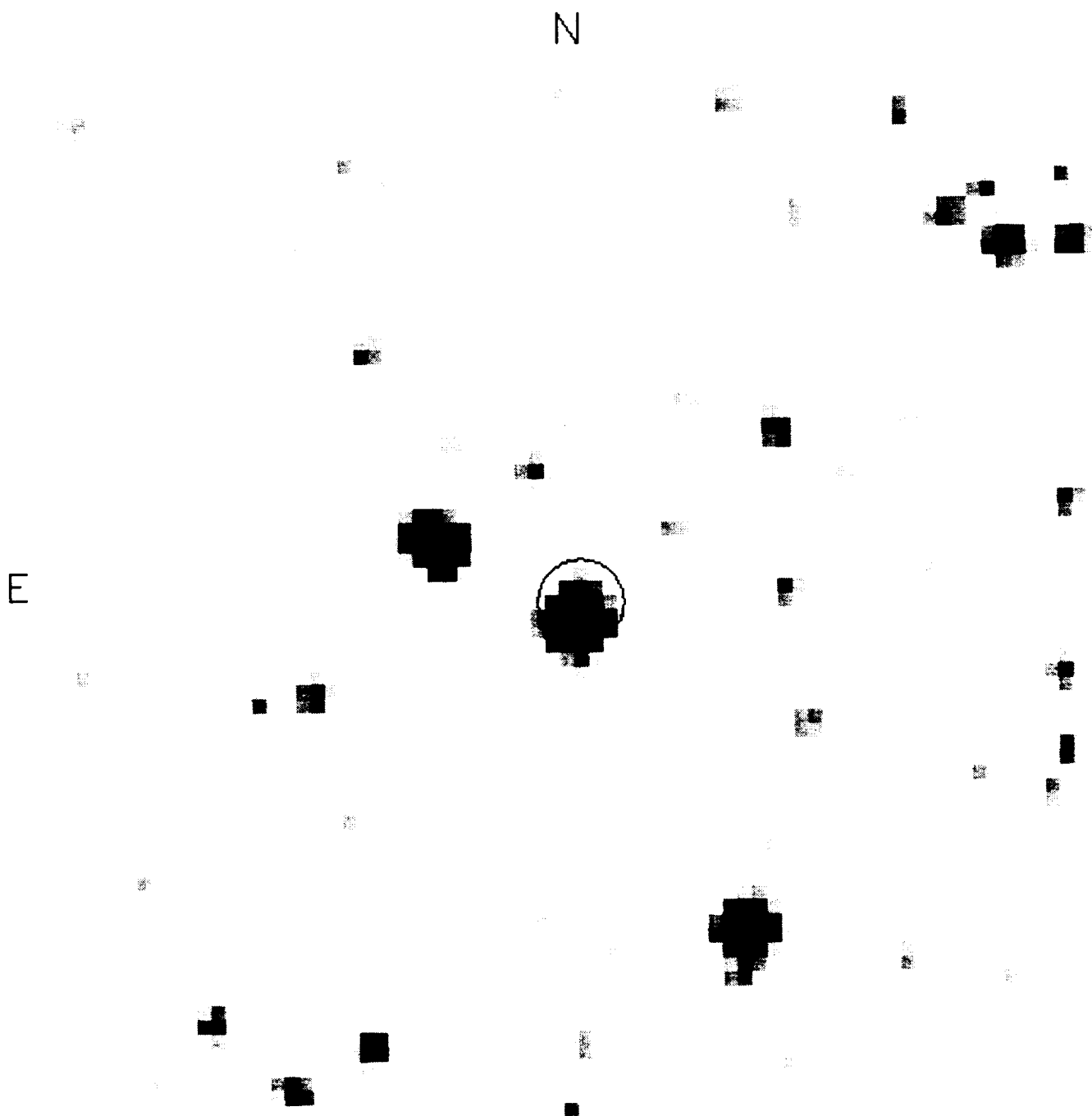
N

E

FIG. 2.—2' × 2' portion of the Digital Sky Survey with the 5" radius error circle of the X-ray position of RX J0117.6−7330

CLARK, REMILLARD, & WOO (see 474, L111)

TABLE 1

UPPER LIMITS ON THE FRACTIONAL AMPLITUDES OF
SINUSOIDAL PULSATIONS IN THE 1992 DATA

			FREQUENCIES (Hz)				
T (s)	M	n	0.1	1.0	10	100	150
400....	18	17	0.10	0.10	0.10	0.12	0.15

the effects on the average rate of variations in the effective detection efficiency for a point source as its image passes over the grid structure of the PSPC window. The count rate varies about the overall average of 3.79 counts s^{-1} on timescales from several minutes to hours. (For comparison, we cite the maximum count rate of SMC X-1, recorded shortly after eclipse egress in the 1992 observation, which was 4.8 counts s^{-1}.)

We searched for evidence of periodic pulsations in the 1992 data by Fourier analysis according to the procedure described by Leahy et al. (1983). The data were divided into M subsets of continuous exposure of length T. Events within the 1.'67 circle were binned in intervals of length $\delta T = T/2^n$. The fast Fourier transform was applied to each of the binned subsets, and the average of the normalized power density (PD) spectra was computed. In the case of $T = 400$ s with $M = 18$, we set $n = 17$. In the frequency range from 0.1 Hz to the Nyquist frequency at 163.84 Hz, the mean and variance of the power density are 2.000 and 0.224, consistent with purely Poisson fluctuations for which the expected mean and variance are 2 and 4/18. The largest PD in that frequency range is $P_{max} = 4.34$. The expected number of PDs greater than 4.34 in a spectrum of Poisson noise is ~3. Thus, there is no evidence of a PD that cannot be attributed to Poisson noise.

In the frequency range below 0.1 Hz, there is a rise in the average PD caused by low-frequency variations in detection efficiency due to the quasi-periodic spacecraft wobble and by nonperiodic variations of the source intensity. The two highest PDs, other than the expected one at 0.0025 Hz, are at 0.0100 and 0.0125 Hz with values of 5.98, and 5.87, respectively. They are also probably caused by the wobble. Discounting these features of the low-frequency PD spectrum, we find no evidence of a source periodicity in the frequency range from 0.01 to 163.84 Hz. In Table 1, we list the estimated 99% confidence upper limits on the fractional amplitudes of sinusoidal variations that would have escaped detection. We derived the limits by analyzing sets of fake data generated with an average count rate of 4 s^{-1}, modulated by sinusoids of various amplitudes and frequencies.

The mean count rate of background-subtracted events in the 1993 data was 0.014 s^{-1}—a reduction by a factor of 270 from the mean rate during the 1992 observation, and too small to allow a significant search for periodicity. The reduction corresponds to an e-folding decay time of 44 days.

2.3. Spectrum

Figure 4b is a plot of the hardness ratios of the 1992 background-subtracted pulse-height distributions (PHD), calculated as the ratio of the average rates in pulse-height channels corresponding to the energy ranges 0.3–1.0 keV and 1.0–2.5 keV. The lack of correlation between changes in the hardness ratio and the count rate indicates that the rate change is caused by variations in the intrinsic luminosity of the source and not by variable absorption.
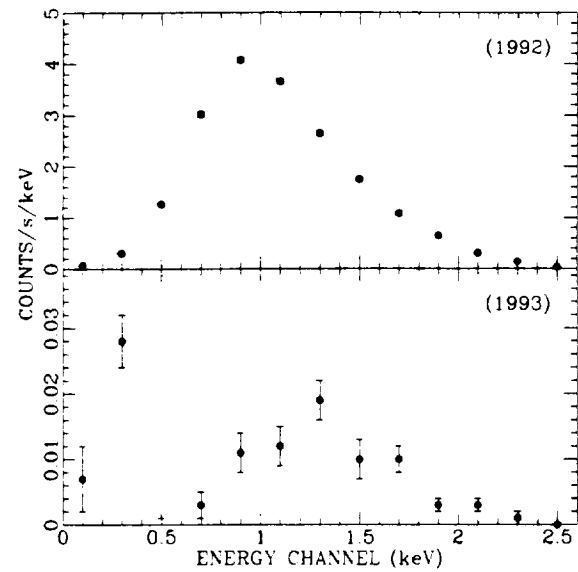

FIG. 5.—Background-subtracted pulse-height distributions from the 1992 and 1993 observations.

The spectrum of the transient as characterized by its hardness ratio is softer than that of SMC X-1; the average value was 1.14 ± 0.02 compared to 1.36 ± 0.01 for SMC X-1 in the 1991 observation of the uneclipsed pulsar. To characterize the spectrum in more detail, we fitted the PHD of the 1992 data (Fig. 5) with various trial spectrum functions. The results are summarized in Table 2. None of the simple trial functions yields a satisfactory fit; neither does the disk blackbody (DBB) model of Mitsuda et al. (1984). Good fits are obtained with a power law added to either a bremsstrahlung function or blackbody function. The latter combination yields the more plausible power-law index and a plausible blackbody temperature. However, the narrow energy range and poor resolution of the spectral data poorly constrain such multiple parameter fits, so no certain conclusion can be drawn regarding the actual presence of a blackbody component. The good fits imply an incident energy flux of (5.3 ± 0.3) × 10^{-11} ergs cm^{-2} s^{-1} in the energy range 0.2–2.5 keV.

The background-subtracted PHD of the 1993 data (Fig. 5), though sparse, shows evidence of a flux below the carbon edge of the detector response at 0.28 keV. To check whether this might be the result of an error in background subtraction, we replaced the concentric annulus background PHD with the PHD of events in a circle of radius 1.'67, centered on a position at the same declination as the transient, and as far west of SMCX-1 as the transient was east of it. No significant difference in the background-subtracted PHD was found. The ratio of the rate in channels corresponding to calibration energies from 0.1 to 0.3 keV to the rate above 0.3 keV is 0.045, whereas the ratio in the 1992 data is 0.0008. Thus, it seems that the proportion of an ultra–low-energy component in the total spectrum increased as the total intensity decayed. To evaluate the incident energy flux, we fitted spectrum functions in the form of a power law plus a blackbody function to the PHD with the column density fixed at 5 × 10^{20} H-atoms cm^{-2}, which is the approximate value implied by the 0.26 mag optical extinction of the nearby Sk 160 (van der Klis et al. 1982). The low-energy (<0.28 keV) and high-energy (>0.28 keV) portions of the PHD can be fitted separately by the tail of a cool

TABLE 2

FITS OF MODEL PHOTON NUMBER SPECTRA TO THE PULSE-HEIGHT DISTRIBUTION OF THE 1992 DATA

Spectrum Form	N_H $(10^{21}$ cm$^{-2})$	Index	kT (keV)	Flux $(10^{-11}$ ergs cm^{-2} s$^{-1})$	χ_ν^2
PE*PL	2.4 ± 0.1	2.7 ± 0.1	...	5.1	2.1
PE*BR	1.5 ± 0.1	...	1.22 ± 0.06	5.0	2.5
PE*BB	0.07 ± 0.04	...	0.299 ± 0.003	4.5	8.0
PE*DBB	1.16 ± 0.05	...	0.467 ± 0.010	4.8	4.2
PE*(PL+BR)	6.9 ± 0.7	6.6 ± 0.5	10*	5.3	1.2
PE*(PL+BB)	1.2 ± 0.2	0.23 ± 0.08	0.21 ± 0.02	5.4	1.3

NOTE.—PE stands for photoelectric absorption; PL means power law; BR means thermal bremsstrahlung; BB is Planck blackbody; DBB is disk blackbody.

* Fixed.

blackbody function with $kT < 0.07$ keV plus a hard power law with index 0, respectively. Alternatively, the low- and high-energy protons can be fitted by a soft power law with index 4 plus a hot blackbody function with $kT = 3$ keV, respectively. Both fits are so poorly constrained that little physical significance can be attached to them. However, they yield consistent, although crude, estimates of the incident flux: in the energy range 0.10–0.28 keV, the flux is $(1.7 \pm 0.5) \times 10^{-15}$ ergs cm^{-2} s^{-1}; and in the entire range 0.10–2.5 keV, it is $(3.4 \pm 0.5) \times 10^{-13}$ ergs cm^{-2} s^{-1}.

3. DISCUSSION

Above 2 mcrab, the occurrence frequency of high-latitude Galactic X-ray transients associated with nearby stars is roughly 1 order of magnitude greater than the frequency of X-ray transients in the Magellanic Clouds. However, given the small solid angle subtended by the SMC, about 2.5×10^{-4} of the celestial sphere, a robust transient observed in the direction of the SMC, such as RX J0117.6–7330, is much more likely to be located in the SMC than in the Galaxy. The absence of a bright, red star near the X-ray position further limits the probability that the X-ray source is a Galactic object. Moreover, within the 5″ radius positional error circle of the X-ray transient there is a likely optical counterpart in the form of a Be star with a magnitude consistent with a location in the SMC. Thus, it appears almost certain that the transient lies in the SMC.

If the transient is at a distance D and radiates isotropically, then the received energy flux implies an average luminosity in the 0.2–2.5 keV range of $\sim 1.6 \times 10^{37}(D/50$ kpc$)^2$ ergs s^{-1} during the 1992 observation, consistent with the typical luminosities of accretion-powered X-ray sources.

The column density of hydrogen in front of the transient during the 1992 observation, although poorly constrained by the data, appears to exceed 1.0×10^{21} cm^{-2}. This is more than

the column density implied by the optical extinction toward nearby Sk 160. The appearance of a component below 0.28 keV in the spectrum of the transient 8 months later suggests that the column density inferred from the 1992 data was of circumstellar matter that dissipated as the transient faded.

Although it seems likely that RX J0117.6–7330 is another example of a neutron star with a Be-type companion, it is worthwhile to consider the possibility that it is a BHXN. Its apparent e-folding decay time of 44 days is within the range typical of BHXN. We have found no evidence of periodic variation. Its spectrum during the 1992 observation was softer than that of SMC X-1, although the narrow energy range of the PSPC precludes a definitive comparison of the transient's spectrum with the characteristics of typical BHXNs. Thus, the apparent decay time, the apparent absence of pulsation, and a spectrum that is substantially softer than the nearby pulsar are consistent with the properties of identified BHXN. To be sure, the likely optical counterpart is not a late-type dwarf or subgiant like the companions of the known BHXN. However, there seems to be no reason, in principle, why the companion of a stellar black hole cannot be a Be star. A determination of the mass function of the system or a more sensitive search for pulsations during a recurrence of an X-ray outburst might settle the question.

REFERENCES

Aschenbach, B. 1988, Appl. Opt., 27, 1404
Charles, P. A., Southwell, K. A., & O'Donoghue, D. 1996, IAU Circ. 6305
Clark, G. W., Remillard, R. A., & Woo, J. W. 1996, IAU Circ. 6282
Hughes, J. P. 1994, ApJ, 427, 25
Kahabka, P., & Pietsch, W. 1996, A&A, submitted
Leahy, D. A., Darbro, W., Elsner, R. F., Weisskopf, M. C., Sutherland, P. G., Kahn, S., & Grindlay, J. E. 1983, ApJ, 266, 160
Mitsuda, K., et al. 1984, PASJ, 36, 741
Pfeffermann, E., et al. 1987, Proc. SPIE, 733, 519
Schmidtke, P. C., Cowley, A. P., McGrath, T. K., & Anderson, A. L. 1995, PASP, 107, 450

Seward, F. D., & Mitchell, M. 1981, ApJ, 243, 736
Tanaka, Y., & Lewin, W. H. G. 1995, in X-Ray Binaries, ed. W. H. G. Lewin, J. van Paradijs, & E. P. J. van den Heuvel (Cambridge: Cambridge Univ. Press), 127
Trümper, J. 1983, Adv. Space Res., 2, 241
van der Klis, M., et al. 1982, A&A, 61, L19
van Paradijs, J. 1995, in X-Ray Binaries, ed. W. H. G. Lewin, J. van Paradijs, & E. P. J. van den Heuvel (Cambridge: Cambridge Univ. Press), 536

ROSAT OBSERVATIONS OF SCATTERED X-RAYS FROM LMC X-4 IN ITS LOW STATE

JONATHAN W. WOO, GEORGE W. CLARK,[1] AND ALAN M. LEVINE

Center for Space Research, Massachusetts Institute of Technology, Cambridge, MA 02139

ABSTRACT

Observations of the eclipsing accretion-powered high-mass X-ray binary LMC X-4 are described that confirm the idea that the low state of its 30.3 day period cyclical intensity variation is caused by a periodic blockage of the line of sight by a precessing accretion disk that is tilted with respect to the orbital plane of the binary. The principal evidence consists of the fact that the intensity and spectrum of scattered X-rays measured during total eclipse of the neutron star by the primary star are approximately the same in both the high and low states of the 30.3 day cycle. Therefore, the low state must be caused not by a decrease in the luminosity of the X-ray source but, rather, by total attenuation in intervening matter. Differences between the spectra observed in and out of eclipse in the high and in the low states are also consistent with the precessing disk hypothesis. The brightest of several flares detected in the low state had a peak intensity, which implies a source luminosity (0.2–2.5 keV) of 4×10^{39} ergs s^{-1} if the measured flux is interpreted as scattered and fluorescent radiation from the primary star's surface illuminated by the unblocked X-ray source. This peak luminosity is comparable to that previously reported for a flare observed in the high state. The flare also showed marginal evidence of the pulsar modulation, which is not inconsistent with the degree of spread in path lengths of the scattered radiation. The data also show that the column density to LMC X-4, derived by spectrum fits in both the low and high states, is about 4 times larger than the interstellar neutral hydrogen column density toward the LMC, possibly as a result of a circumstellar accumulation of matter from the wind of the primary.

Subject headings: accretion, accretion disks — binaries: eclipsing — stars: individual (LMC X-4) — X-rays: stars

1. INTRODUCTION

When the neutron star in a high-mass accretion-powered X-ray binary is eclipsed by the primary star, one can generally detect a residual intensity of X-rays that are the secondary Compton-scattered and fluorescent radiation from the stellar wind of the primary. Since the matter in the wind is widely distributed and broadly illuminated by the neutron star, it is reasonable to assume that the intensity of this secondary radiation is proportional to the intrinsic luminosity of the neutron star and, therefore, approximately constant. An interesting complication can arise if there is sufficient interstellar dust along or near the line of sight to give rise to grain-scattered X-rays that are delayed in arrival at Earth by virtue of their greater path lengths. The grain-scattered X-rays may then constitute a significant portion of the eclipse intensity in the form of an X-ray halo (Clark, Woo, & Nagase 1994, and references therein). In the case of an X-ray binary in the Magellanic Clouds, however, the column density of interstellar dust along the line of sight is so small that grain-scattered X-rays constitute a negligible fraction of the X-rays detected during an eclipse. Thus, essentially all the X-rays detected during an eclipse are secondary radiation, the intensity of which can be taken as a measure of the intrinsic luminosity of the eclipsed neutron star.

LMC X-4 is an eclipsing high-mass accretion-powered X-ray binary in the Large Magellanic Cloud with the properties listed in Table 1. Its intensity varies by a factor of ~60 between high and low states with a periodic cycle time of 30.3 days. This long-term variation, like the long-term variation of Her X-1,

[1] Department of Physics, Massachusetts Institute of Technology, Cambridge, MA 02139.

has been attributed to blockage of the direct X-ray beam by a precessing accretion disk that is tilted with respect to the orbit plane of the binary and periodically lies in a plane containing the line of sight to the neutron star (Lang et al. 1981; Priedhorsky & Holt 1987, and references therein). Dennerl et al. (1992) studied the long-term variation of LMC X-4 in the ROSAT All-Sky Survey data and in the EXOSAT data and concluded that the period is slowly decreasing. Features of the optical light curve have also been interpreted in terms of a precessing accretion disk (Ilovaisky et al. 1984; see also Heemskerk & van Paradijs 1989). A geometric model of the system has been devised by Heemskerk & van Paradijs (1989).

About once per day LMC X-4 exhibits a "flaring episode" during which the intensity increases sporadically by factors of up to ~20 for times ranging from ~20 s to 45 minutes (Epstein et al. 1977; White 1978; Skinner et al. 1980; Kelley et al. 1983; Pietsch et al. 1985; Dennerl 1989; Levine et al. 1991). The average spectrum ($E > 1$ keV) during a flaring episode is much softer than the average spectrum at other times.

In this paper we describe observations of LMC X-4 in and out of eclipse that prove that the low state of the long-term variation is caused by blockage of the line of sight to the neutron star as implied by the model of a precessing accretion disk. The observations also show changes in the X-ray spectrum in and out of eclipse and provide data on the intensity and modulation of a giant flare in the low state, which can be understood in terms of the model. The data also yield a measure of the thickness of circumstellar matter surrounding LMC X-4.

The observations are described in § 2, and the data analysis is given in § 3. Interpretation of the analysis and discussion of the binary properties of LMC X-4 are presented in § 4.

Parameter	Value	Reference
P_{orb}	1.40841 days	1
i_c (inclination angle)	57°– 65°	2
M_{opt}/M_X	10.6	2
θ_e (eclipse half-angle)	21°– 25°	2
R_0 (primary radius)	8.1 $R_\odot$	2
P_{pulse}	13.50 s	1
L_{opt}	6×10^{38} ergs s^{-1}	3
S_p	O7 III–V	3
A_V	0.16 mag	4
Distance	55 kpc	5

NOTE.—(1) Levine et al. 1991; (2) Woo 1993; (3) Hutchings, Crampton, & Cowley 1978; (4) van der Klis et al. 1982; (5) adopted.

2. OBSERVATIONS

We obtained data from two observations of LMC X-4 made with the Position Sensitive Proportional Counter (PSPC) in the focal plane of the X-ray telescope (XRT) of the X-ray observatory *ROSAT* (Trümper 1983). The PSPC-XRT system (Pfeffermann et al. 1987; Aschenbach 1988) was sensitive to X-rays in the energy range from 0.1 to 2.4 keV and had a field of view of 57′ radius. The energy resolution of the PSPC was 45% FWHM at 1 keV. The PSPC-XRT system efficiently rejected charged particle events and provided ~25″ angular resolution.

The first observation was carried out from 1991 October 28.6 to November 3.6 and yielded 46,000 s of useful data. Its purpose was to observe the northern part of the Large Magellanic Cloud; LMC X-4 was located about 40′ away from the image center (Bomans, Dennerl, & Kürster 1994). The second observation was from 1992 July 9.2 to 10.7 with a total exposure of 14,500 s with LMC X-4 close to the center of the field of view.

We estimated the phase of the long-term variation during each of the observations from the period and epoch given by Dennerl et al. (1992). These authors reported a light curve of LMC X-4 over ~40 days based on *ROSAT* sky survey data and found an epoch of maximum intensity (phase 0.0) of JD 2,448,226.0. They derived a period of ~30.25 ± 0.03 days from a combined analysis of *ROSAT* and much earlier *EXOSAT* data. Using this ephemeris (which differs in the definition of zero phase from that of Lang et al. 1981), we found that the interval 1991 October 28.6 to November 3.6 corresponds to phases in the range from ~ −0.05 to ~0.15 with an uncertainty of ~0.01, which is in the high-intensity state of the cycle. The observation of 1992 July 9–10 spanned phases from 0.36 to 0.41 with an uncertainty of 0.02, during which LMC X-4 is in its low-intensity state.

3. DATA ANALYSIS AND RESULTS

For both observations, source counts were taken from a circular region centered on the image of LMC X-4, while background count rates in the source region were estimated from appropriately scaled count rates obtained in an annular region of the image surrounding the source region.

In the 1991 observation, the image of LMC X-4 was relatively large because of the off-axis aberrations of the XRT. We therefore defined the source region to have a radius of $r < 4.5$ around the image center of LMC X-4 and defined the background region by $6' < r < 8'$. Only events in pulse-height chan-

nels 20–249 (0.2–2.5 keV) were used. The source region data were corrected for background and then for vignetting using the exposure map of the entire observation.

For the 1992 observation, the source region was defined to have a radius of 1′ around the image center of LMC X-4, while background estimates were obtained from a source-free annulus defined by $(1.7 < r < 4.2)$. Only events in pulse-height channels 20–247 (0.2–2.48 keV) were selected for the rest of our analysis. These selection criteria yielded an estimated background rate of 4×10^{-4} counts s^{-1} arcmin^{-2} keV^{-1} within this energy band, which is consistent with its being dominated by cosmic X-ray–induced events. The source region data were corrected for background, but no vignetting corrections were applied.

3.1. X-Ray Light Curves and Pulsations

The count rates in 216 s time bins for both the high- and low-intensity state observations are shown in Figures 1 and 2, respectively. In the high-intensity state the typical out-of-eclipse count rate was 6–8 counts s^{-1}, and the average in-eclipse count rate was 0.030 ± 0.006. The latter is about 0.5% of the out-of-eclipse intensity, which is consistent with the results from a previous observation of LMC X-4 with the *Ginga* satellite (Woo 1993).

During most of the observation in the low-intensity state the out-of-eclipse count rates were low (~0.1 counts s^{-1}) but nonetheless higher than the average in-eclipse count rate of 0.023 ± 0.004 counts s^{-1}. There were also two intervals of flaring activity lasting several thousand seconds during which the count rates increased suddenly, briefly, and sporadically. The flaring episodes are marked "FL01" and "FL02." Figure 2c displays the hardness ratio defined as the ratio of the count rates above and below 0.5 keV. The plot shows that the spectrum hardened during the flaring episodes.

The intervals containing flares are replotted in Figure 3 with finer time resolution. Figures 3a and 3b show several flares that consist of sudden increases in count rates to levels about 5 times the average between flares with durations of several hundred seconds. Similar flares were observed with *Ginga* (Levine et al. 1991). The strongest flare during the second episode is displayed in Figure 3c with a time resolution of 1 s. The peak count rate (~30–40 counts s^{-1}) was several hundred times the average count rate outside of the flaring episodes (~0.1–0.2 counts s^{-1}).

In Figure 2, we have marked the expected X-ray eclipse intervals with thick lines and the letters "EC." The average count rate around orbital phase 0.5 was approximately 6 times the average in-eclipse count rate.

A search for pulsations yielded evidence of periodic modulation with a statistical significance of about 2 σ in 200 s of data during the giant flare. The modulation is most significant at a trial period of 14.5 s.

3.2. Spectral Analysis

We constructed average background-subtracted pulse-height distributions (PHDs) from the uneclipsed high- and low-state data, in the following three categories: (1) data recorded during the flaring episodes displayed in Figure 2 (FL01 and FL02); (2) data recorded during the largest flare displayed in Figure 3c; (3) data not included either in category (1) or in the eclipses (EC). For each PHD in the energy range from 0.2 to 2.48 keV, we fitted a model PHD derived as a convolution of the PSPC response matrix with the following
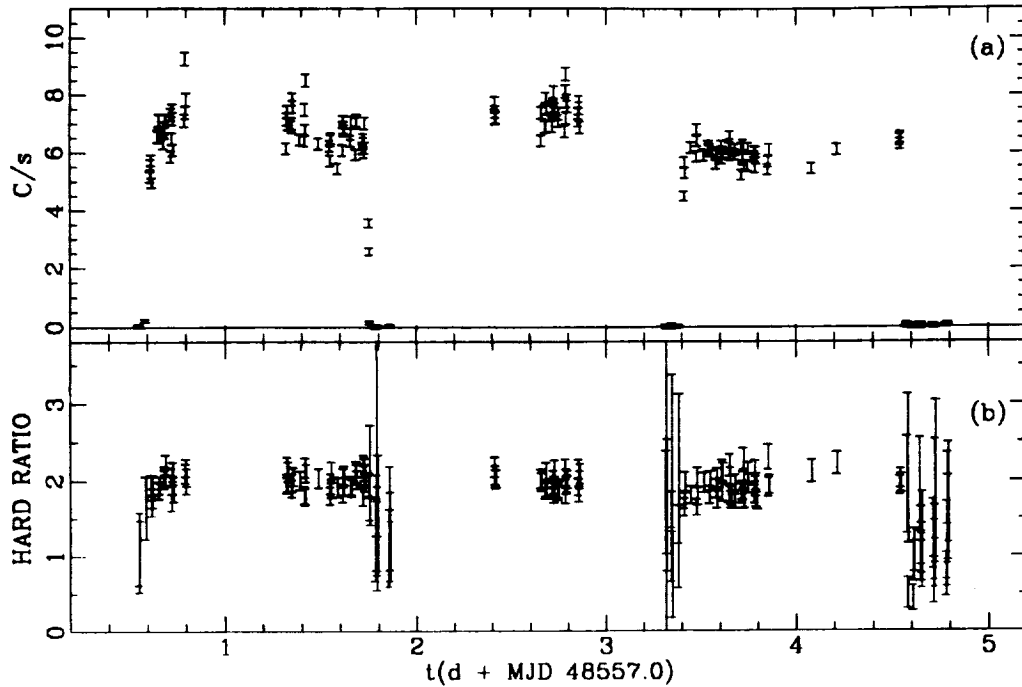
FIG. 1.—(a) *ROSAT* PSPC light curve of LMC X-4 (216 s bins) observed in the high-intensity state (1991 Oct 28.6–Nov 3.6). (b) The ratio of the count rate above 0.5 keV to that below 0.5 keV.

spectrum function expressed as photons cm^{-2} s^{-1} keV^{-1} and composed of an absorption factor multiplied by the sum of three component spectra: two power-law components and a Planck function:

$$I(E) = \exp\left[-\sigma(E)N_H\right]$$

$$\times \left[I_{pl1}E^{-\alpha_1} + I_{pl2}E^{-\alpha_2} + I_{bb}\left(\frac{E}{E_{bb}}\right)^2 \frac{(e-1)}{\exp(E/E_{bb}) - 1}\right]. \quad (1)$$

I_{bb} is the blackbody intensity at $E = E_{bb}$, I_{pl1} and I_{pl2} are the power-law intensities at $E = 1$ keV, and e is the base of the natural logarithms. The shape parameters are the blackbody temperature E_{bb} and the power-law indices α_1 and α_2. The first power-law component represents the radiation from the accretion disk and is expected to be characterized by a higher value of α than the second power-law component. The second power-law component represents the radiation from the accretion column of the neutron star. Because of the falloff in sensitivity of the *ROSAT* PSPC-XRT above 2.5 keV, the power-law components were not well constrained. We therefore forced the index α_2 of the power law that we associate with the accretion column component to be 0.6, based on the previous *Ginga* observations of LMC X-4 (Levine et al. 1991; Woo 1993). The X-ray absorption cross section was assumed to be $\sigma(E) = \sigma_{ph}(E) + 1.21\sigma_T$, where $\sigma_{ph}(E)$ is the photoelectric absorption cross section of cold matter given by Morrison & McCammon (1983), σ_T is the Thomson scattering cross section, and the factor 1.21 is the number of electrons per proton in the absorbing matter with normal cosmic abundances. A blackbody component with $E_{bb} = 0.16$ keV was first detected in an analysis of *Einstein* solid state spectrometer observations of SMC X-1 by Marshall, White, & Becker (1983) and later in the analyses of *ROSAT* and *Ginga* observations of SMC X-1 by Woo et al. (1995).

For the spectrum fitting we rebinned the 256 channel PHDs accumulated from high-state data into 34 channels and the low-state PHDs into bins with at least 30 counts. The best-fit spectral parameters for the four average PHDs are listed in Table 2, and the fitted PHDs are shown in Figure 4.

From the optical extinction, $E(B-V) = 0.05 \pm 0.02$ mag, determined by Bonnet-Bidaud et al. (1981), the interstellar column density toward LMC X-4 is about 3×10^{20} H atoms cm^{-2} (Zombeck 1990). The absorption column densities derived from the spectral fits for all four spectra are much larger, which may signify a local accumulation of circumstellar matter.

3.3. Monte Carlo Simulation

To aid in the interpretation of the X-ray light curve, we carried out a Monte Carlo calculation of the propagation of X-rays through a spherically symmetric X-ray–ionized atmosphere with parameters adjusted to model the LMC X-4 primary star. The code was the same as that used in a previous study (Woo 1993). For the atmospheric density function we adopted the "hybrid" function from Clark et al. (1994):

$$n(r) = \frac{\Psi}{4\pi\mu r^2}\left\{1 + \left(\frac{r}{r_1}\right)^2\left(1 - \frac{r_0}{r}\right)^\beta \exp\left[-\frac{(r-r_1)}{h}\right]\right\}$$

$$\times \left(1 - \frac{r_0}{r}\right)^{-\beta}, \quad (2)$$

in which $\Psi = \dot{M}/v_t$ represents the ratio of the mass-loss rate to the terminal velocity of the stellar wind. The quantity r_0 is an effective radius of the primary star that we set equal to the value 5.59×10^{11} cm. We adjusted the values of Ψ, β, r_1, and h, which were initially adopted from the *Ginga* LMC X-4 study (Woo 1993), to match the predicted light curve of the scattered photons in the Monte Carlo simulation with the observed X-ray light curve.
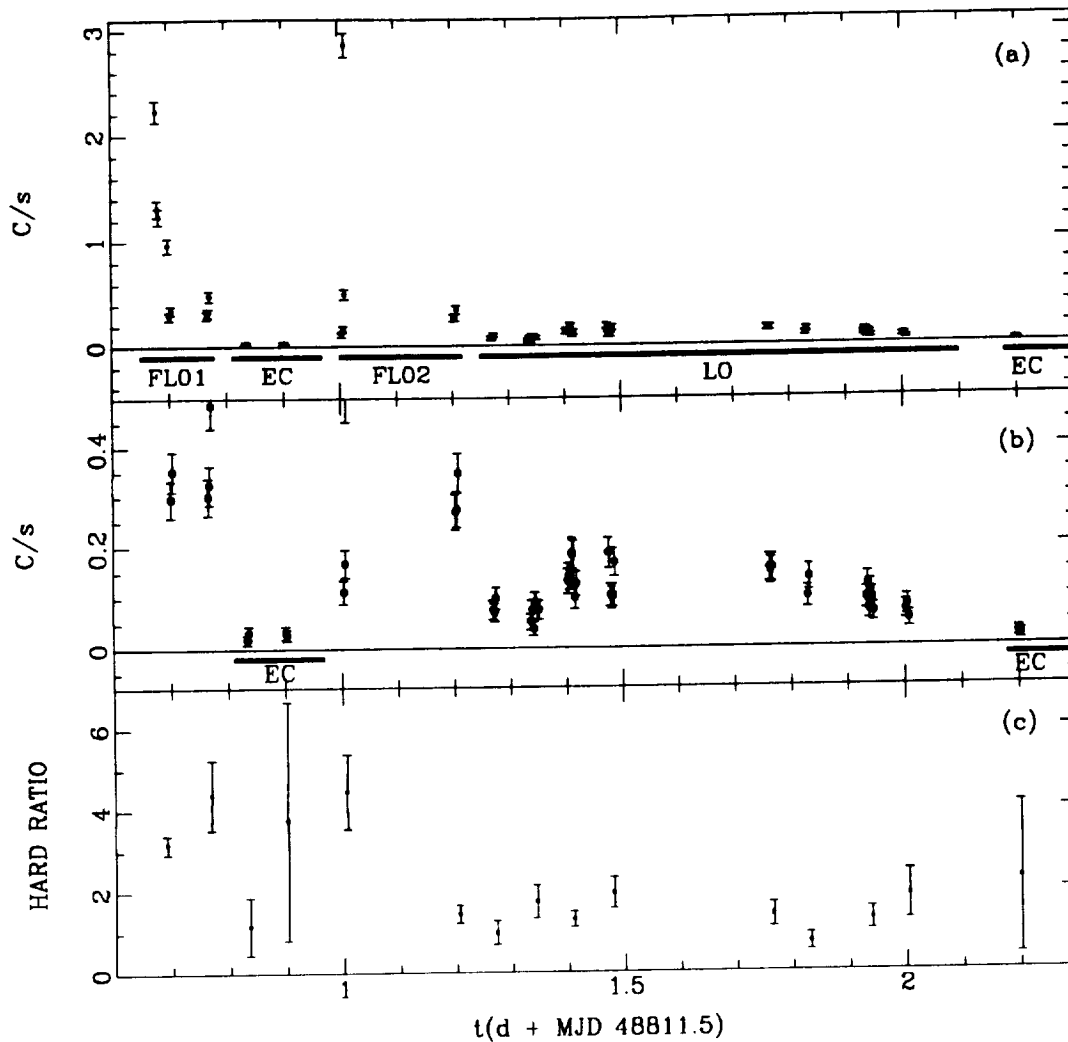
Fig. 2.—(a) ROSAT PSPC light curve of LMC X-4 (216 s bins). (b) The same light curve as in (a) but with an expanded count rate scale. (c) The ratio of the count rate above 0.5 keV to that below 0.5 keV. In (a) the time intervals that were used to construct the four spectra are shown: "FL01," "EC," "FL02," and "LO." Predicted eclipse intervals are marked as "EC" in (b).

We assumed that the photoelectric absorption cross section at a given location at a given energy is determined by the local ionization parameter $\xi = L_X/(nr^2)$. The local ionization parameter was calculated a priori by propagating the source spectrum through the atmosphere with the density function of equation (2). The Monte Carlo code launches 1 keV X-ray photons from the neutron star in random directions. Each photon is tracked in steps of 1/10 or less of a mean interaction length. At each interaction site, the photon may be Compton scattered or photoelectrically absorbed. If the photon is Compton-scattered, a new energy and direction for the scattered photon are calculated. If the photon is photoelectrically

TABLE 2

FITTED VALUES OF THE SPECTRAL FUNCTION

Parameter	High	Low	Flaring Episodes	Giant Flare
$N_H (10^{20}$ cm^{-2})	12.9 (0.7)	16.7 (12.7)	10.4 (7.1)	2.4 (0.5)
α_1	8.4 (0.4)	9.0 (6.7)	8.5 (5.3)	
I_{pl1} (photons keV^{-1} cm^2 s^{-1})	4.2E$-$4 (1.7E$-$4)	0.17E$-$4 (1.32E$-$4)	0.13E$-$4 (1.11E$-$4)	
α_2[a]	0.6	0.6	0.6	0.6
I_{pl2} (photons keV^{-1} cm^2 s^{-1})	0.0117 (0.0003)	1.26E$-$4 (1.87E$-$4)	0.0027 (0.0003)	0.023 (0.004)
E_{bb} (keV)	0.154 (0.003)	0.16 (0.12)	0.15 (0.02)	0.16 (0.02)
I_{bb} (photons keV^{-1} cm^2 s^{-1})	0.22 (0.02)	0.0020 (0.0081)	0.046 (0.046)	0.20 (0.02)
χ_v^2	1.39	0.35	0.65	0.52
F_X[b] $(10^{-10}$ ergs cm^2 s^{-1})	0.99	0.016	0.17	1.75

NOTE.—The 1 σ uncertainties are quoted within the parentheses.
[a] The parameter value is fixed.
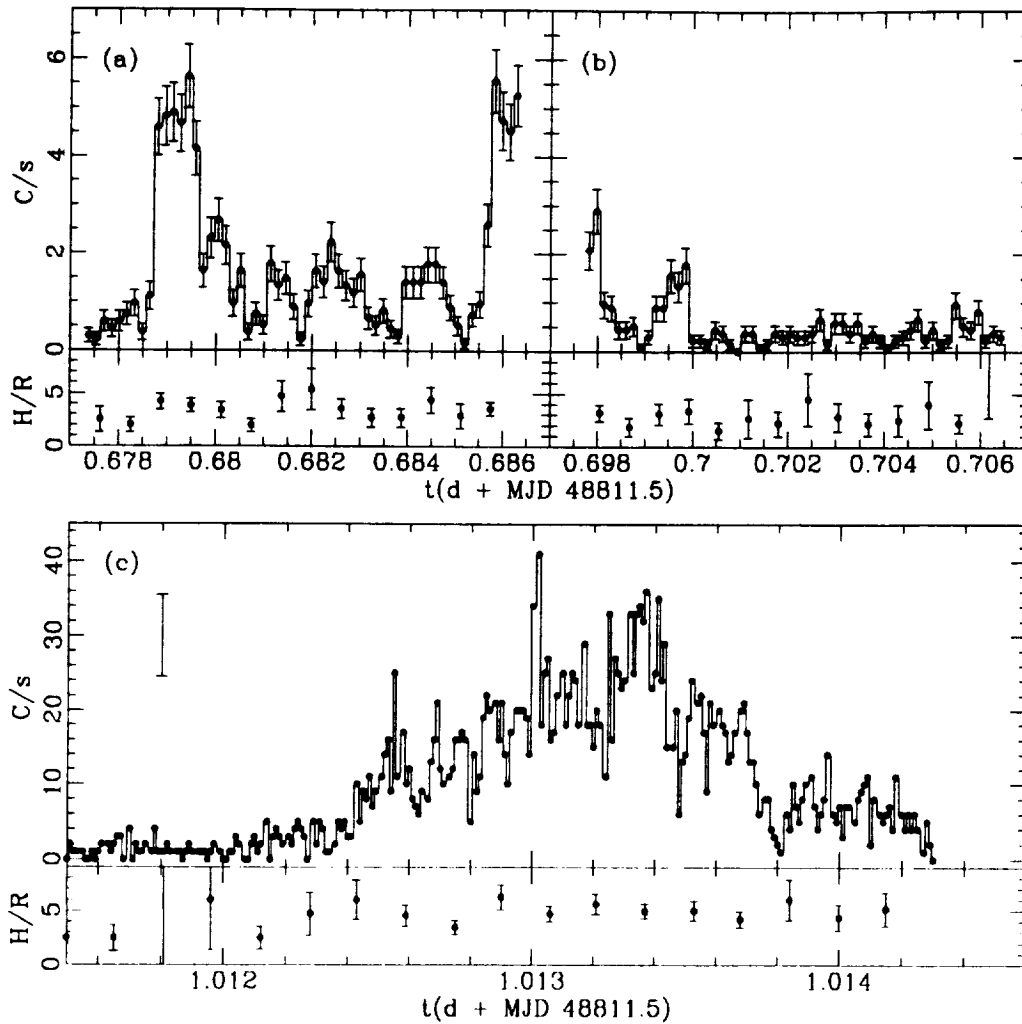[b] For $0.2 < E < 2.5$ keV.

FIG. 3.—Details of light curves and hardness ratios during flares: (a) and (b) show 13.5 s data bins, and (c) shows 1 s data bins (to show short time variabilities). In (c), a typical ± 1 σ error bar due to counting statistics is shown (for 30 counts s⁻¹).

absorbed, there may be fluorescent emission from iron or lower Z elements that are taken to be present with normal cosmic abundances.

The adjusted values of the hybrid density function parameters are $\Psi = 1.0 \times 10^{-10}\ M_\odot\ \mathrm{yr}^{-1}\ \mathrm{km}^{-1}$ s, $\beta = 1$, $r_1 = 1.41r_0$, and $h = 2.82 \times 10^{10}$ cm.

Figure 5 displays the fraction of the 1 keV X-ray photons that are scattered at least once before escaping from the binary system. The scattering fraction varies from ~0.5% at the eclipse to ~3% around orbital phase 0.5. Out of eclipse the interactions are mostly Compton scattering from the stellar surface, so that the variation in the X-ray–illuminated area of the companion star visible from Earth produces an orbital phase–dependent intensity variation.

4. DISCUSSION

We have found that the X-ray intensities of LMC X-4 in eclipse during the low and high states are approximately the same. In striking contrast, the out-of-eclipse intensities differ by a factor of about 60 between the low and high states. Since the X-rays observed in eclipse are scattered from widely spread circumsource matter, their intensity provides a fair measure of the intrinsic luminosity of the neutron star. The similarity of the in-eclipse intensities in the high and low states therefore proves that the cause of the 30.3 day high-low cycle is not variations in the intrinsic X-ray luminosity of the neutron star. Instead, the cause must be periodic blockage of the line of sight to the neutron star. This conclusion is reinforced by the fact that the low-state out-of-eclipse intensity varies with orbital phase in a manner consistent with the Monte Carlo–calculated light curve of X-rays scattered by circumstellar matter and by the X-ray–illuminated surface of the primary star. Finally, the low-state out-of-eclipse spectrum is consistent with that expected for scattered and fluorescent radiation. All these results support the explanation of the long-term high-low variation of the X-ray intensity as the result of a periodic blockage of the line of sight by an accretion disk that is tilted with respect to the orbital plane and that precesses with the period of the high-low cycle.

Adopting a distance to LMC X-4 of 55 kpc, assuming isotropic scattering from circumstellar matter as the secondary source of X-rays observed during the low state, and using the measured flux cited in Table 2, we find the average luminosity (0.2–2.5 keV) of scattered radiation to be 5.8×10^{35} ergs s⁻¹ during the uneclipsed, nonflaring low state. According to the Monte Carlo calculation (see Fig. 5), which assumes that the
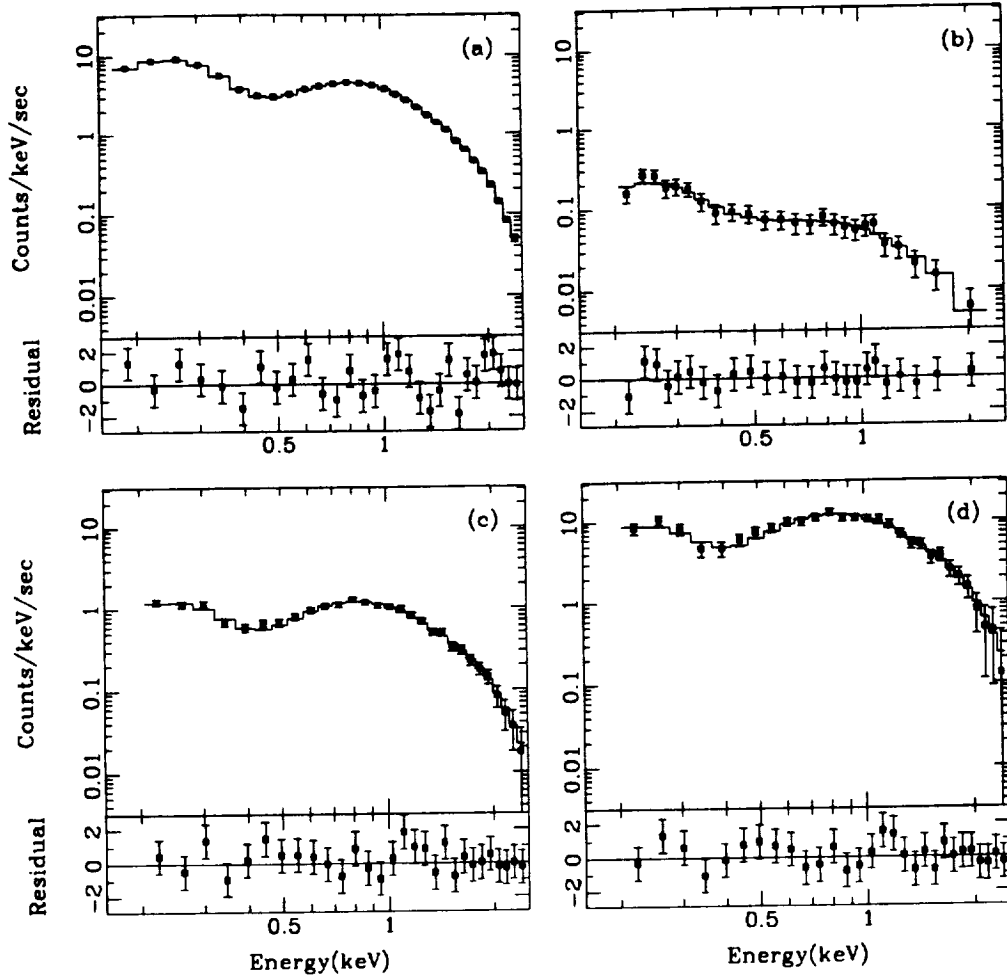
FIG. 4.—Pulse-height distributions of LMC X-4: (a) uneclipsed high state, (b) uneclipsed low state, (c) flaring episodes, and (d) the largest single flare (~200 s interval over flare shown in Fig. 3c). Histograms represent the best-fit pulse-height distributions.
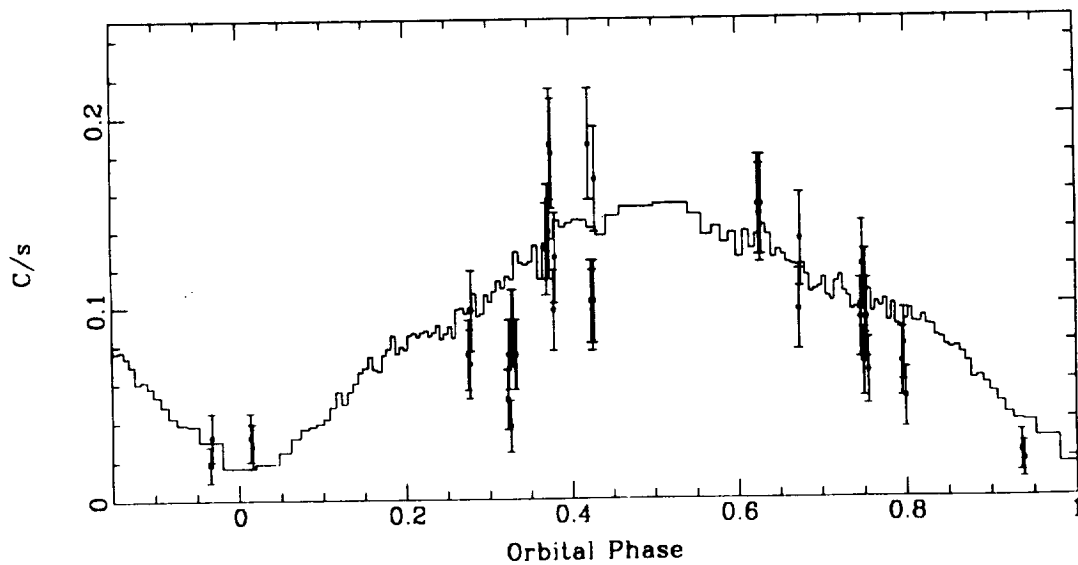

FIG. 5.—The observed count rates and predicted scattered-radiation light curve (histogram) that has been scaled to the observed light curve are plotted as a function of the orbital phase. A count rate of 0.1 counts s⁻¹ corresponds to 2% of the unobscured direct intensity observed during the high state.

neutron star radiates isotropically, this luminosity is ~3% of the source luminosity; therefore, the implied intrinsic source luminosity must have been $\sim 2 \times 10^{37}$ ergs s^{-1}. At the peak of the giant flare (Fig. 3) the count rate is ~ 30 count s^{-1} or about 200 times higher than the count rate in the quiescent state (~ 0.15 count s^{-1} in Fig. 5). We can rule out the possibility that the flare X-rays were detected through the accretion disk because the measured column density is consistent with the circumstellar column density determined from the high-state data. It follows that the intrinsic source luminosity (0.2–2.5 keV) at the peak of the flare was approximately 4×10^{39} ergs s^{-1}, much larger than the Eddington limit. A similar high luminosity was found at the peak of a flare in the high state in a *Ginga* observation (Levine et al. 1991). Thus, the circumstellar matter responsible for scattering the X-rays in our direction must have been exposed to the full flare intensity of the neutron star.

If the apparent 14.5 s modulation in the giant flare data is real, then it must be a modulation in the intensity of the pulsar X-rays scattered from matter close enough to the line of sight to the neutron star to avoid complete smearing in time due to path length differences. When the neutron star is out of eclipse but hidden by the accretion disk, the surface of the primary is illuminated and, therefore, a source of albedo X-rays. The light travel time from the neutron star to the subsatellite point on the primary's surface is 11 s, comparable to the pulse period. Thus, it is reasonable to expect some remnant of the pulse modulation to be present in the scattered radiation. In fact, the giant flare occurred just after the neutron star emerged from eclipse so that only a thin crescent of the X-ray–illuminated surface of the primary was exposed to Earth. In that configuration the path length spread and the resultant reduction in the fractional pulse modulation are minimized. We note that the pulse fraction observed in the high state by *Ginga* (Levine et al. 1991) was ~0.5 during the intense flares compared to ~0.1 during quiescence. The apparent pulse fraction of ~0.2, which we obtain for the large flare in the low state, is smaller than in the previously observed high-state flares. The difference between the observed period and the intrinsic pulsar period may be an effect of the rapid changes of the source intensity during the flare or possibly a change in the beaming pattern as has been observed previously (e.g., Levine et al. 1991).

We note that changes in beaming pattern of the X-ray pulsar, as opposed to changes in luminosity, would not, except in very contrived situations, affect the scattered flux by a large factor. Therefore, the flares must be caused by large intrinsic changes in neutron star X-ray luminosity.

In a study of the distribution of circumstellar matter in a model of the high-mass X-ray binary SMC X-1, carried out by numerical three-dimensional hydrodynamic computation, Blondin & Woo (1995) demonstrated that X-ray heating of the primary star's atmosphere drives a thermal wind that constitutes most of the matter that populates the circumstellar environment. Quantitative estimates of the resulting column density of this circumstellar matter provided a plausible expla-

nation for the excess of the column density to SMC X-1 over the interstellar column density derived from optical observations. The excess column density over the amount attributable to the interstellar medium in the present case of LMC X-4 also suggests an accumulation of circumstellar material from the wind of the primary star.

In thinking about possible future observations, we note that there is a large difference in the relative contributions to the spectrum of scattered X-rays observed in and out of eclipse from distant circumstellar matter and from matter near the primary's surface in systems like LMC X-4. Since the ionization state of the matter in these two scattering regimes may be quite different because of the difference in density and associated recombination rates, one can expect to observe differences in the relative intensities of the fluorescent lines in and out of eclipse, particularly during the low state when the direct beam is blocked. Such differences may be detectable with the improved spectrometry capabilities of future X-ray observatories and could provide interesting new information about the state and distribution of circumstellar matter in high-mass X-ray binaries.

The principal results of the present study can be summarized as follows:

In both the low and the high states of LMC X-4, the ratios of the in-eclipse intensities to the intensity at orbital phase 0.5 in the high-state were the same within the uncertainties of measurement and were approximately 0.005. In addition, the spectra out of eclipse in both the low and the high state were similar in shape.

The low-state out-of-eclipse intensity was ~3% of the high-state out-of-eclipse intensity. The low-state light curve is consistent with that predicted by a Monte Carlo calculation of scattering and fluorescence in the atmosphere and wind of the companion star, which is under X-ray illumination by the neutron star emitting at the same level of intrinsic luminosity as in the high state.

These results support the idea that the low-intensity state is caused by periodic blocking of the line of sight to the neutron star by an accretion disk that is tilted with respect to the orbital plane.

Two flaring episodes were observed, separated by ~10 hr. Individual flares showing count rate increases by at least 1 order of magnitude typically lasted several hundred seconds.

The column density to LMC X-4 determined from data accumulated during both low and high states is about 4 times larger than the interstellar column density of $N_H^{ISM} = 3 \times 10^{20}$ H atoms cm^{-2} inferred from optical measurements. The excess column density may indicate an accumulation of matter from the thermal wind driven from the surface of the primary star by X-ray heating.

REFERENCES

Aschenbach, B. 1988, Appl. Opt., 27, 1404
Blondin, J. M., & Woo, J. W. 1995, ApJ, 445, 889
Bomans, D. J., Dennerl, K., & Kürster, M. 1994, A&A, 283, L21
Bonnet-Bidaud, J. M., Ilovaisky, S. A., Mouchet, M., Hammerschlag-Hensberge, G., van der Klis, M., Glencross, W. M., & Willis, A. J. 1981, A&A, 101, 184
Clark, G. W., Woo, J. W., & Nagase, F. 1994, ApJ, 422, 336

Dennerl, K. 1989, in Proc. 23d ESLAB Symp., ed. J. Hunt & B. Battrick (Noordwijk: ESA-ESTEC), 39
Dennerl, K., Kuerster, M., Pietsch, W., & Voges, W. 1992, in Lecture Notes in Physics, Vol. 416, New Aspects of Magellanic Cloud Research, ed. B. Baschek, G. Klare, & J. Lequeux (Berlin: Springer), 74
Epstein, A., Delvaille, J., Helmken, H., Murray, S., Schnopper, H., Doxsey, R., & Primini, F. 1977, ApJ, 216, 103

Heemskerk, M. H. M., & van Paradijs, J. 1989, A&A, 223, 154
Hutchings, J. B., Crampton, D., & Cowley, A. P. 1978, ApJ, 225, 548
Ilovaisky, S. A., Chevalier, C., Motch, C., Pakull, M., van Paradijs, J., & Lub, J. 1984, A&A, 140, 251
Kelley, R. L., Jernigan, J. G., Levine, A., Petro, L. D., & Rappaport, S. 1983, ApJ, 264, 568
Lang, F. L., Levine, A. M., Bautz, M., Hauskins, S., Howe, S., Primini, S. A., Lewin, W. H. G., Baity, W. A., Knight, F. K., Rothschild, R. E., & Petterson, J. A. 1981, ApJ, 246, L21
Levine, A., Rappaport, S., Putney, A., Corbet, R., & Nagase, F. 1991, ApJ, 381, 101
Marshall, F. E., White, N. E., & Becker, R. H. 1983, ApJ, 266, 814
Morrison, R., & McCammon, D. 1983, ApJ, 270, 119
Pfeffermann, E., et al. 1987, Proc. SPIE, 733, 519

Pietsch, W., Pakull, M., Voges, W., & Staubert, R. 1985, Space Sci. Rev., 40, 371
Priedhorsky, W. C., & Holt, S. S. 1987, Space Sci. Rev., 45, 291
Skinner, G. K., et al. 1980, ApJ, 240, 619
Trümper, J. 1983, Adv. Space Res., 2, 241
van der Klis, M., Hammerschlag-Hensberge, G., Bonnet-Bidaud, J. M., Ilovaisky, S. A., Mouchet, M., Glencross, W. M., Willis, A. J., van Paradijs, J. A., Zuiderwijk, E. J., & Chevalier, C. 1982, A&A, 106, 339
White, N. E. 1978, Nature, 271, 38
Woo, J. W. 1993, Ph.D. thesis, MIT
Woo, J. W., Clark, G. W., Blondin, J. M., Kallman, T. R., & Nagase, F. 1995, ApJ, 445, 896
Zombeck, M. V. 1990, Handbook of Space Astronomy & Astrophysics (Cambridge: Cambridge University Press)